

A Model for Predicting Pipeline Sinkage Induced by Tunnel Scour

Chengcai Luo¹, Hongwei An², Liang Cheng³ and David White⁴

^{1,2,3}*School of Civil and Resource Engineering, the University of Western Australia, Perth, Australia*

⁴*Centre for Offshore Foundation Systems, the University of Western Australia, Perth, Australia*

¹*E-mail: chengcai.luo@uwa.edu.au*

ABSTRACT: The current design practice for subsea pipeline on-bottom stability (e.g. DNV-RP-F109) does not account the effect of sediment transport around a pipeline. Both field survey and small scale model test results show that seabed scour has a significant effect on pipeline embedment and therefore stability. Physical model tests carried out in an innovative large experimental facility, named the O-tube, at the University of Western Australia, have shown that tunnel scour and the subsequent pipe sinkage into the scour hole tend to stabilize a pipeline which might otherwise become unstable on an assumed stationary seabed, under ramping-up flow conditions. A simple calculation model that incorporates the three-dimensional scour and pipe sinkage due to the soil bearing capacity failure at the supporting span shoulders is proposed. The model parameters were calibrated using the O-tube experimental results. The model serves as a key element of a new pipeline stability analysis method that takes into account seabed mobility.

KEYWORDS: Pipeline, On-bottom stability, Tunnel scour, Pipe sinkage

1. INTRODUCTION

The total length of subsea pipelines being installed and planned for transporting oil and gas worldwide is increasing rapidly with the ongoing development of offshore oil and gas extraction activities. On-bottom stability is one of the key issues for maintaining pipeline integrity. Although the practice of submarine pipeline on-bottom stability design has been developed since the 1950s, there are still major uncertainties in this subject. For instance, the effect of seabed mobility on pipeline stability, although observed in practice, has still not been considered in the pipeline stability analysis. It has been pointed out that significant sediment transport could take place long before the pipe starts to move (Palmer, 1996). The commonly used offshore pipeline stability design method DNV-RP-F109 design code itself states that ‘by these formulae [with regard to seabed stability], it may be shown that non-cohesive soil will in many cases become unstable for water velocities significantly less than the velocity that causes an unstable pipe’.

Seabed scour around pipelines, as a major seabed mobility form, changes the pipe embedment conditions and therefore its stability. Tunnel scour and pipeline free-span have been given particular attention in the last few decades. The initiation of tunnel scour could be induced by an uneven seabed or the piping mechanism. The piping (seepage failure) is due to the pressure gradient exceeding the effective weight of non-cohesive sand particles (Mao 1988, Chiew 1990). Sumer et al. (2001) carried out physical experiments to investigate the onset of tunnel scour of a shallowly embedded model pipe under steady current and wave actions. An empirical equation was given to determine the critical current velocity under a specific embedment ratio. Zang et al. (2009, 2010) developed a numerical model to simulate the onset of tunnel scour. By examining the pressure gradient around the invert part of the pipe, a novel equation to predict the onset velocity under oscillatory and combined flow conditions was given. More recently, Gao and Luo (2010) investigated the onset of tunnel scour experimentally and numerically. The results indicated that the critical onset velocity increases with the internal friction angle of sediment. Once the tunnel gap is opened, scour develops downwards and propagates laterally along the pipeline. Free-span of a pipeline forms following the 3D scour process. A comprehensive summary about scour hole shapes and the time scale for scour development under different flow conditions can be found in Sumer and Fredsøe (2002). 3D scour under both current, wave and combined flow condition was also investigated by Cheng et al. (2009, 2013) and a method to assess the lateral scour rate along the pipeline has been proposed.

As the scour propagates along the pipeline, the length of the supporting soil shoulder shortens gradually, and additional vertical

load is transferred to the pipe resting at the shoulders. As a result, the pipeline might lower into the seabed due to bearing capacity failure of the soil shoulders. Meanwhile, pipeline deflection may occur over a sufficiently long free-span section. Which of the two scenarios occurs depends on the distribution of the free-spans along the pipeline and the relative stiffness of the pipeline compared to the strength of seabed soils at span shoulders. Pipeline sinkage into the scour hole changes the pipeline-seabed configuration and therefore affects pipeline on-bottom stability, due to the variation of the hydrodynamic loading and the pipe-soil resistance. Until now, little work has been done to link the development of scour and the subsequent pipe sinkage, which affects pipeline stability.

To investigate the effect of seabed scour on pipeline stability under realistic storm conditions, an innovative experimental facility, called the O-tube, was established at the University of Western Australia (UWA). The O-tube facility is capable of simulating near seabed hydrodynamic conditions induced by cyclonic storms at seabed level so that the response of pipelines and model seabed can be revealed in a relatively large scale (An, et al. 2013). A range of pipeline dynamic stability tests under varying flow conditions were carried out in the O-tube. In this paper, several typical test results were presented to demonstrate the effect of seabed scour on pipeline stability. Based on the existing scour knowledge and the O-tube test findings, a model incorporating the scour development and pipe sinkage due to soil failure was proposed. The model parameters were calibrated using the O-tube test results. The application of this model was also briefly discussed.

2. PHYSICAL MODEL TESTS

2.1 Testing facility: The Large O-tube

The Large O-tube (LOT) is a large closed loop flume, as shown in Figure 1, developed at the University of Western Australia for investigating the ocean-structure-seabed interaction. The water in the O-tube is circulated by an axial pump system to generate various flow conditions, including steady currents, oscillatory flows, combined currents and oscillatory flow and irregular storm conditions. The generated oscillatory velocity amplitude can be up to 2.5 m/s at period of 13s and 1m/s at period of 5s. Given the large performance envelope of the O-tube flume, it is capable of simulating the hydrodynamic conditions induced by cyclonic storm at seabed level so that the response of seabed sediment and any infrastructure that is resting on it can be revealed at a relatively large scale. Detailed information of the O-tube facility is given by An, et al. (2013) and the calibration of the O-tube facility is given by Luo et al. (2012).

An instrumented model pipe connected with an actuator system was developed to test the stability of a model pipeline in the LOT, as shown in Figure 2. The diameter of the model pipe is 196mm and the total length of the model pipe is 990mm. The model pipe is instrumented with two load cells and eighteen pore pressure transducers (PPTs). The actuator system was designed for the control of the model pipe. The actuator control system not only restrains unrealistic rotation of the model pipe through the rigid connection of the two actuator arms, but also eliminates the interference from the control system to the model pipe through the feedback control so that the pipe can move ‘naturally’ in response to hydrodynamic loads and the soil resistance. The operation of the actuator and the O-tube were computerized through UWA-designed control software (De Catania et al. 2010), and all data acquisition was achieved using UWA-designed DAQ units (Gaudin et al. 2009).

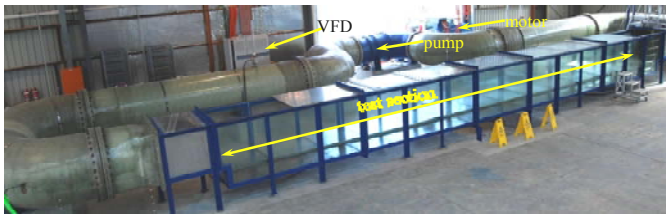


Figure 1. UWA's Large O-tube (LOT) flume.

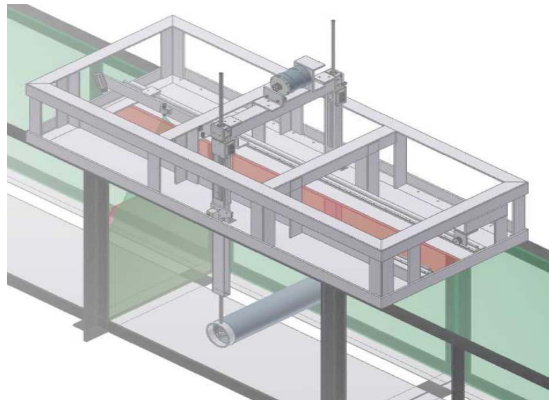


Figure 2. Schematic of the actuator and model pipe.

Apart from the model pipe and actuator, other main apparatus include Acoustic Doppler Velocimeter (ADV) for measuring the flow velocity, seabed profilers for measuring seabed profiles, pore pressure transducers to measure pore pressure variations in the model seabed. The model seabed was installed on the bottom of the test section, midway through the whole test section.

2.2 Test conditions

2.2.1 Model pipe setup

In the present work, the model pipe was tested on an initially flat model seabed and was controlled to simulate a specific gravity (SG) of 1.5. Although a very small embedment was achieved due to the self-weight of the model pipe, the tests were defined as ‘zero’ embedment condition. During the test, the model pipe was maintained under load control in both horizontal and vertical direction through the actuator system. In horizontal direction, the controlled target force was set as zero, which allowed the model pipe to respond to the hydrodynamic force and soil resistance in a natural way. In vertical direction, the load was maintained to simulate the pipe SG.

2.2.2 Seabed model and sediment property

The dimension of the model seabed was 6m in length, 1m in width and 0.2m in depth. A brick-paved false floor was used for the rest of the test section, beyond the 6 m length. The water depth above the model seabed was 1.2m, reaching to the lid of the flume.

The sediment used in the tests was carbonate sand with >80% calcium carbonate content. The key physical properties of the calcareous sediment are: submerged soil unit weight = 9.06kN/m³, particle density = 2.77·10³kg/m³ and median particle size = 0.2mm. The particle size distribution (PSD) from sieve and sedimentation analysis is shown in Figure 3.

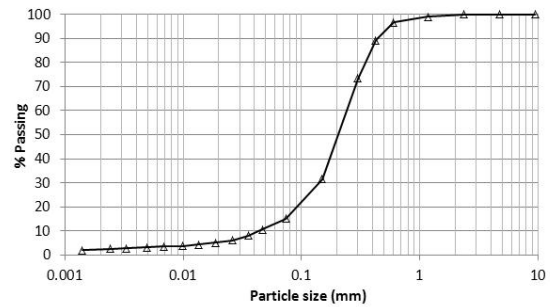


Figure 3. PSD curve of the model seabed soil.

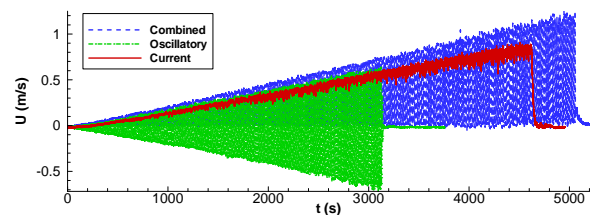
2.2.3 Flow conditions

Pipeline stability and seabed mobility are highly dependent on the flow conditions. One of the key parameters in the flow conditions is the flow ramp-up rate, as seabed sediment often starts to move at a flow velocity significantly lower than that required to destabilise the pipeline. Also, seabed scour is an accumulated process which takes place in a larger time-scale, comparing with the process of a pipeline losing stability (which is an event associated with a single wave). To investigate the effect of seabed scour on pipeline stability, a slow flow ramp-up rate of 0.0002m/s² was employed. This ramp-up rate is representative of a typical storm at Australia's North West Shelf.

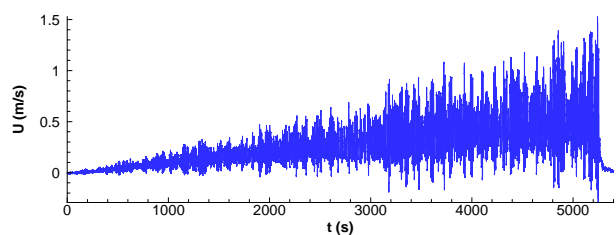
Four cases with the slow ramp-up rate were presented in this paper. The flow conditions are (i) current, (ii) regular oscillatory flow, (iii) combined regular oscillatory flow and current and (iv) irregular combined flow, respectively. The flow conditions were summarized in Table 1. The measured velocity time series for the four cases are shown in Figure 4.

Table1. Flow conditions

| No. | a _c (m/s ²) | a _s (m/s ²) | m | T (s) | Comments |
|-----|------------------------------------|------------------------------------|---|-------|-------------------------|
| 1 | 2E-4 | 0 | ∞ | - | Current |
| 2 | 0 | 2E-4 | 0 | 10 | Oscillatory flow |
| 3 | 1E-4 | 1E-4 | 1 | 10 | Combined flow |
| 4 | 1E-4 | 1E-4 | 1 | 10 | Irregular combined flow |



(a) Current, regular oscillatory and combined flow



(b) Irregular combined flow

Figure 4. Measured flow velocity time-series.

2.3 Test results

The test results showed that under the ramp-up flow conditions, the model pipe experienced sinkage induced by tunnel scour. The pipe trajectories of the four cases are shown in Figure 5. Except for the oscillatory flow condition case, where the pipe moved laterally (>1D) to the motion limit of the test setup, for all of the other three cases the pipe sank into the scour hole and reached the bottom of the test section without being destabilised. The different stability behaviour under oscillatory flow and other flow conditions were mainly attributed to the different hydrodynamic forces. Although the peak flow velocity was ramped up at almost the same rate over time, the flow accelerations for the three cases (current, oscillatory and combined flow) were different. Therefore, the inertia forces of the three flow conditions differed, as did the horizontal hydrodynamic forces. The measured hydrodynamic forces under the three flow conditions are shown in Figure 6. It is observed that the force amplitude induced by the oscillatory flow at a given time instant was larger than those induced by the combined flow and the steady current, especially the lift force at time instants M1 and M2.

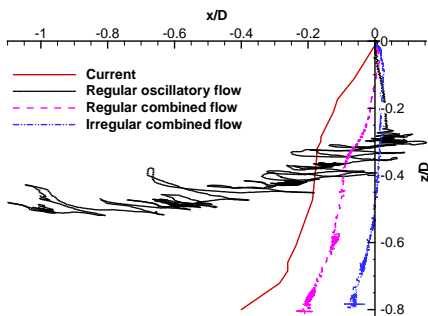


Figure 5. Pipe trajectories.

The flow velocity reached over 1m/s at the end of the tests for the two combined flow cases. In the absence of seabed mobility, the pipe would have lost stability at a flow of ~0.56 m/s, based on estimated drag and friction values.

This paper focuses on the time development of pipe sinkage (z), which is defined as the pipe elevation below the original far field mudline, with the positive direction being upwards. Where the pipe is partially buried, z is (minus) the pipe embedment (or penetration).

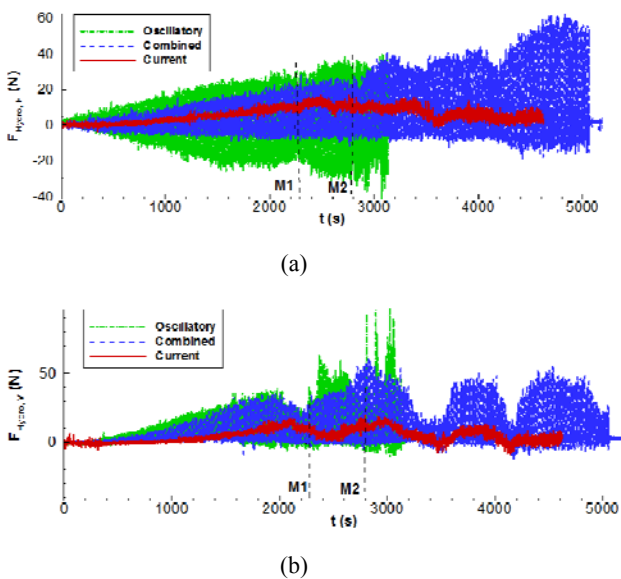


Figure 6. Comparison of hydrodynamic forces under different flow conditions (a) horizontal force; (b) vertical force

Some details regarding how tunnel scour and the subsequent pipe sinkage evolved for the regular combined flow (case 3) are first presented. It was observed from the side glass wall that tunnel scour was initiated when the peak flow velocity was ~0.18m/s. The scour hole deepened continuously with the increase of the flow velocity and the pipe started to sink at around 2200s when the flow velocity was 0.44m/s. At the end of the test, the pipe sank close to the bottom of the test section and the peak flow velocity was around 1.3m/s. A set of photographs of seabed and pipe profiles taken from the side wall of the test section are shown in Figure 7.

The time development of the pipe sinkage depth and scour depth (defined as the distance from the initial seabed surface to the deepest point of scour hole) are shown in Figure 8 for case 3. The scour rate (i.e. increase of depth with time) remained approximately constant from $t = 1000s$ to $4000s$. This feature of the scour hole development differs from published work on scour development under a fixed pipe, which shows a decreasing scour rate over time. This difference is for two reasons. Firstly, the decreasing scour rate is based on tests with a constant flow velocity whilst in the present test the velocity was increasing. Secondly, the pipe sinkage in the present test did not fully close the gap but resulted in a reduced tunnel gap and, therefore, a higher flow velocity in the gap compared to that for a fixed pipe (Dalir, 1996). As the pipe sinks, ‘chasing’ the scour hole, the rate of scour depth increase is maintained.

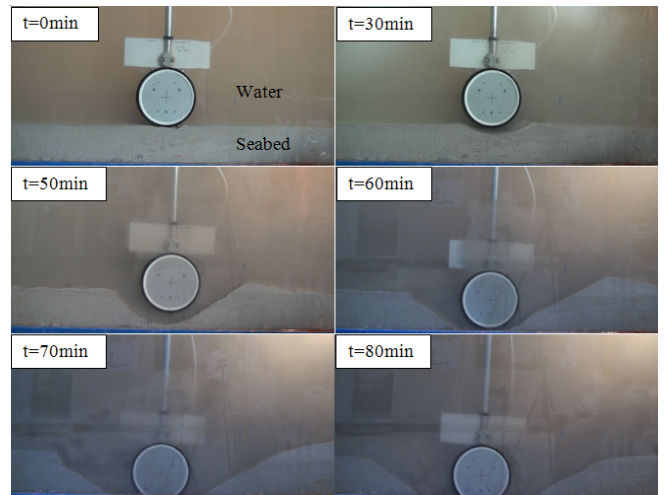


Figure 7. Seabed profile and pipe movement (Case 3) (the current direction was from left to right).

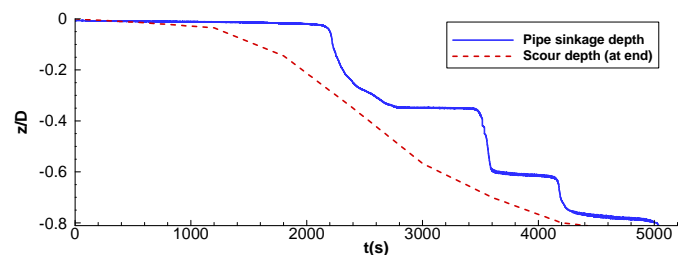


Figure 8. Pipe sinkage and scour depth development (Case 3).

3. MODELLING TUNNEL SCOUR AND PIPE SINKAGE

The pipe sinkage time scale is crucial for determining pipeline stability. In this section, a method for modelling the development of tunnel scour and pipe sinkage is proposed, based on the experimental findings and available scour and pipe-soil vertical interaction knowledge.

3.1 3D scour

The relationship for the current velocity at the onset of scour from Sumer et al. (2001) was employed in this model, which is

$$\frac{U_{cr}^2}{gD(1-n)(s-1)} = 0.025 \exp\left[\theta\left(-\frac{z}{D}\right)^{0.5}\right] \quad (1)$$

where U_{cr} is the critical velocity for the onset of scour, n is soil porosity, s is soil particle density and z is the elevation of the pipe relative to the original seabed surface. For wave conditions, a correction factor of 0.5 was introduced on the right side Eq. (1). For combined wave and current flow condition, a correction factor of 0.8 was introduced on the right side Eq. (1), based on the experimental results from Sumer and Fredsøe (2002).

The 2D tunnel scour time development can be expressed by

$$S = S_{\infty} \left(1 - \exp\left(-\frac{t}{T_s}\right)\right) \quad (2)$$

in which S is the scour depth (below the original mudline) at time t , S_{∞} is the equilibrium scour depth and T_s is the characteristic time-scale (Sumer and Fredsøe, 2002). The calculation of S_{∞} under current only conditions given by Whitehouse (1998) and under wave and combined wave and current conditions by Sumer and Fredsøe (2002) were employed. The characteristic time-scale (T_s) from Fredsøe et al. (1992) was adopted, which is

$$T_s = A\theta^B \frac{D^2}{(g(s-1)d^3)^{1/2}} \quad (3)$$

where θ is the Shield's parameter, d is the median particle size. The coefficients $A = 0.02$ and $B = -5/3$.

Calculation methods for Shield's parameter under different flow conditions and the critical Shield's parameter (θ_{cr}) can be found in Soulsby (1997).

The 2D scour rate can be derived via differentiation of Eq. (2), which gives the vertical erosion rate (v_v) as

$$v_v = \frac{1}{T_s} (S_{\infty} - S) \quad (4)$$

It should be noted that the 2D scour development model was originally developed for pipe that is at a fixed vertical position. However, the pipe in the present tests experienced sinkage as the scour hole deepened. For a scour hole shallower than a certain value, the pipe sinkage reduced the tunnel gap and resulted in an increase in the flow velocity in the gap and therefore an increase in the bed shear stress. As such, v_v under a sinking pipe is accelerated compared to that under a fixed pipe. To account for the effect of pipe sinkage on the acceleration of the vertical erosion rate, the gap distance between the pipe and the seabed (G) was employed in Eq. (4), in place of the scour depth (S), where $G = (S+z)$. In addition, v_v decreases with the increase of the pipe sinkage depth, due to more flow being deflected to the top side of the pipe as the pipe sinks into scour hole. To account for this effect, a correction factor of $1 + z/D$ was introduced to Eq. (4), such that v_v is factored down by an amount which increases linearly to zero when the pipe crown is level with the original seabed surface. The modified 2D scour rate is therefore

$$v_v = \frac{1}{T_s} (S_{\infty} - G) \left(1 + \frac{z}{D}\right) \quad (5)$$

The horizontal scour rate under combined wave and current conditions is taken as (Cheng et al., 2014)

$$v_h = K_{wc} \left(1 + \frac{z}{D} \sin(\tilde{\theta})\right) \sqrt{\frac{g \left(\frac{\rho_s}{\rho} - 1\right) d_{s0}^3}{D \tan \phi}} \frac{((1-m)\theta_w + m\theta_c)^{5/3} F}{(1-m)\theta_w + m\theta_c} \quad (6)$$

where v_h is the horizontal scour propagation rate along the pipeline and K_{wc} is a factor accounting for additional scour mechanisms that may contribute to the scour propagation. According to the

experimental calibration, K was 14 and 4 respectively for the primary and secondary propagation rates under current only condition. In the model, $K=14$ applied to the duration before the pipe starts to sink and $K=4$ applied during the pipe sinkage. α is the flow incident angle, which was zero for the O-tube tests (flow perpendicular to the pipe). Φ is the angle of repose of the soil and assumed to be 45 degree in this case.

By performing time-stepping calculations, the scour depth and span length can be obtained according to the vertical and horizontal scour rates. Based on the current pipe-soil configuration, the hydrodynamic loads on the pipeline can be estimated. The lift force is used to obtain the vertical pipe-soil contact force, which is associated with the pipe penetration depth. As the model is primarily for simulating the pipe sinkage development, the hydrodynamic load was calculated by Morison equations for simplicity, with the force coefficients and load reduction factors due to free-span and penetration from the DNV-RP-F105 (2006) and DNV-RP-F109 (2010) codes, respectively.

3.2 Pipe sinkage - bearing capacity failure of soil shoulders

The pipeline sinkage depth can be estimated based on soil bearing capacity failure. Westgate, et al. (2012) proposed an equation that links the pipe penetration depth (z) and the pipe-soil vertical contact force (V_s) to the seabed penetration resistance (q_b) as

$$q_b = \frac{V_s}{C} \quad (7)$$

where C is the pipe soil contact width, taking into account the local embedment increase due to the heave mounds, as shown in Figure 9. C is related to the pipe embedment as

$$C = \min\left(2D \sqrt{-\frac{1.5z}{D} - \left(\frac{1.5z}{D}\right)^2}, D\right) \quad (8)$$

Based on CPT results performed on the O-tube seabed soil, it was found that the penetration resistance (q_b) increases linearly with penetration depth ($-z$), with the gradient of k_{vp} .

$$q_b = -k_{vp} \cdot z \quad (9)$$

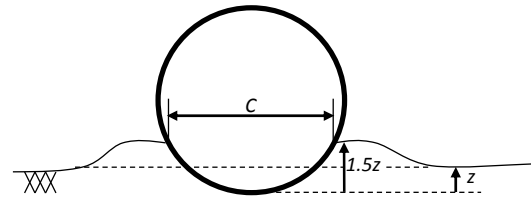


Figure 9. Schematic of pipe-soil contact width.

It should be noted that Eq. (7) is applicable to 2D plane strain conditions. For the pipe-soil contact condition at span shoulders, the length of the shoulder might be comparable to the pipe-soil contact width. In this scenario, the behaviour is no longer 2D. As there is no restraint of the soil in the longitudinal direction, the penetration resistance will be smaller than that in 2D condition. Therefore, the penetration response was modified, based on the O-tube test results, as described in Section 3.4.

3.3 Flowchart

The flowchart for estimating the development of scour depth and pipe sinkage depth is shown in Figure 10. In this model, the pipe is simplified into a single span and shoulder (or two spans adjacent to a single shoulder – which is essentially the geometry of the O-tube tests). The pipe is taken as rigid. The simplifications are suitable for the current work of verifying and calibrating the model elements, based on the O-tube results. In future the model will be extended to more general pipeline conditions.

The time-varying flow condition and the sediment properties are defined first to determine the scour parameters for the pipeline, including their variation with the flow condition. Based on the initial embedment and the initial variation in flow condition, the onset of tunnel scour can be predicted. Once a tunnel is initiated, the erosion rates in both horizontal and vertical direction are calculated. At the same time, the bearing pressure on the span shoulder is determined. Once the bearing capacity is exceeded, the model pipe drops into the scour hole. As this proceeds, the erosion rate and hydrodynamic force is updated based on the embedment depth. Meanwhile the stability criteria are checked. If the pipe is stable in the current time step, the above procedure is repeated in the next time step. Otherwise, the computation is terminated due to pipe breakout.

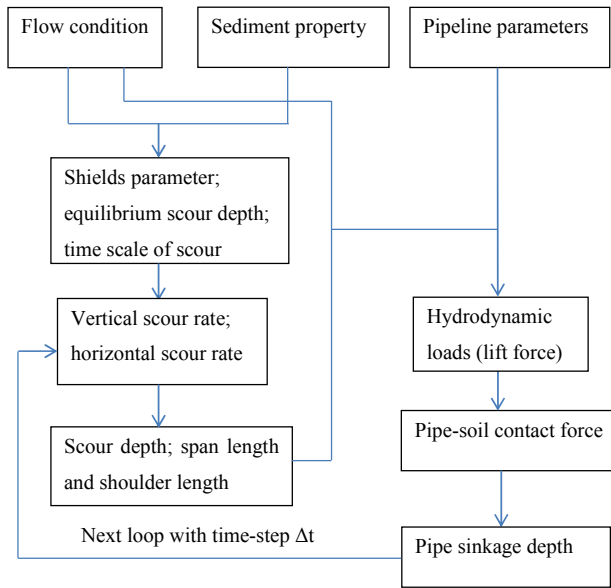


Figure 10. Flowchart of pipe sinkage development model.

3.4 Model parameters and results

The vertical scour rate (v_v) is dependent on the time scale (T_s), in which A and B are experimental fitting parameters. As the test conditions in the present work were different from tests in other published work, especially in that the pipe experiences lowering into the scour hole, the two parameters, A and B , were determined through a model calibration. The same value of $A = 0.02$ to that from Fredsøe et al. (1992) was employed, while the value of B was chosen as -1.2 through calibration. The larger value of B reflects the effect of pipe sinkage on the acceleration of the scour development.

The number for onset of scour points (n) is another parameter that determines the scour propagation rate and therefore the pipe sinkage. Due to the randomness of the onset of scour, it was hard to determine this parameter. In the model calibration, $n=1$ was used.

Seabed penetration resistance (q_b) is a key parameter in this model as it determines the timing of pipe sinkage which in turn affects the scour development rate. The penetration resistance of the pipe can be linked to the tip resistance in a cone penetration test (CPT). However, the value from a CPT test cannot be applied directly to the model, because of the 3D effect at the short span shoulders. The penetration resistance will decrease as the span shoulder shortens. To take into account the 3D effect of resistance reduction at span shoulders, a linear reduction in the penetration resistance gradient when the span shoulder length falls below $5D$ was adopted:

$$k_{vp} = k_{vp0} \cdot L_{sh}/(5D) \text{ for } L_{sh} < 5D \quad (10)$$

where L_{sh} and D are the shoulder length and pipe diameter respectively. For the span shoulder length larger than $5D$, it was

assumed that the 3D effect is negligible, i.e. $k_{vp} = k_{vp0}$ for $L_{sh} \geq 5D$. The model pipe length in the O-tube tests was $5D$, so Eq. (10) applies in the model calibration. The penetration resistance gradient at the start of the test (k_{vp0}) was calibrated using the pipe sinkage time development of the four cases presented above. It was found that $k_{vp0} = 500\text{kPa/m}$.

Using these input parameters and the calculation flowchart in section 3.3, the simulated time development of the scour depth, span shoulder length, pipe-soil vertical contact pressure and the pipe sinkage depth under the combined regular wave and current flow condition of test case 3 is shown in Figure 11. It is seen with the increase of the scour depth, the span shoulder shortens and the pipe-soil contact pressure increases. As a result of the soil bearing failure, the pipe sinkage increases. It is noted in the shoulder length development that before the instant of the pipe suddenly sinking, the shoulder length reduced to a value that is larger than zero, which means the gradient of soil strength in Eq. (10) would always above zero.

It should also be noted in the time-series of shoulder length that following each pipe sinkage, the shoulder length increases to a value close to the pipe length. This value is set to be 99% of the pipe length in the model. This indicates that after each pipe sinkage, the tunnel gap was not fully closed and therefore the scour could keep developing, which is consistent with the observations from the tests.

The measured pipe sinkage time development of the four cases presented in the previous sections were employed for the model validation. The simulated scour depth and pipe sinkage depth from the model were compared with the measured pipe sinkage depth, as shown in Figure 12. It is seen that the model results captured the general trend of the pipe sinkage under different flow conditions. In general, for wave and combined flow conditions, the modelled pipe sinkage was in line with the test results except for some time lags. The time lag of the modelled results can be modified through adjusting the number of onset of scour point that affects the scour propagation rate, and the soil strength that is related to the time when the soil failure (pipe sinkage) occurs. The scour propagation rate might also be varying during the pipe sinkage due to the change of the free-span number. Given the uncertainty of the scour propagation and the penetration resistance, the modelled the pipe sinkage development is reasonably well.

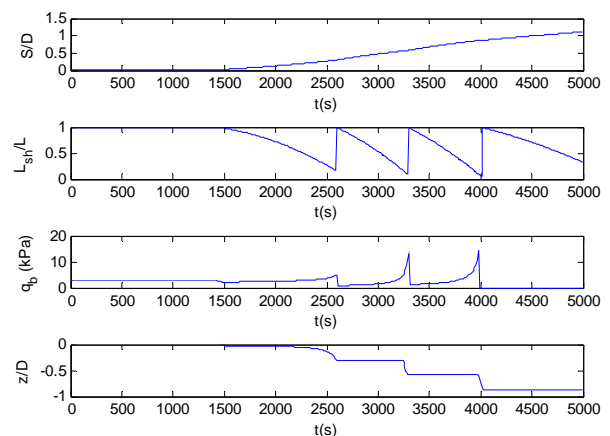


Figure 11. Simulated time-series for scour depth, span shoulder length, pipe-soil contact pressure and pipe sinkage depth for regular combined flow condition (test No. 3)

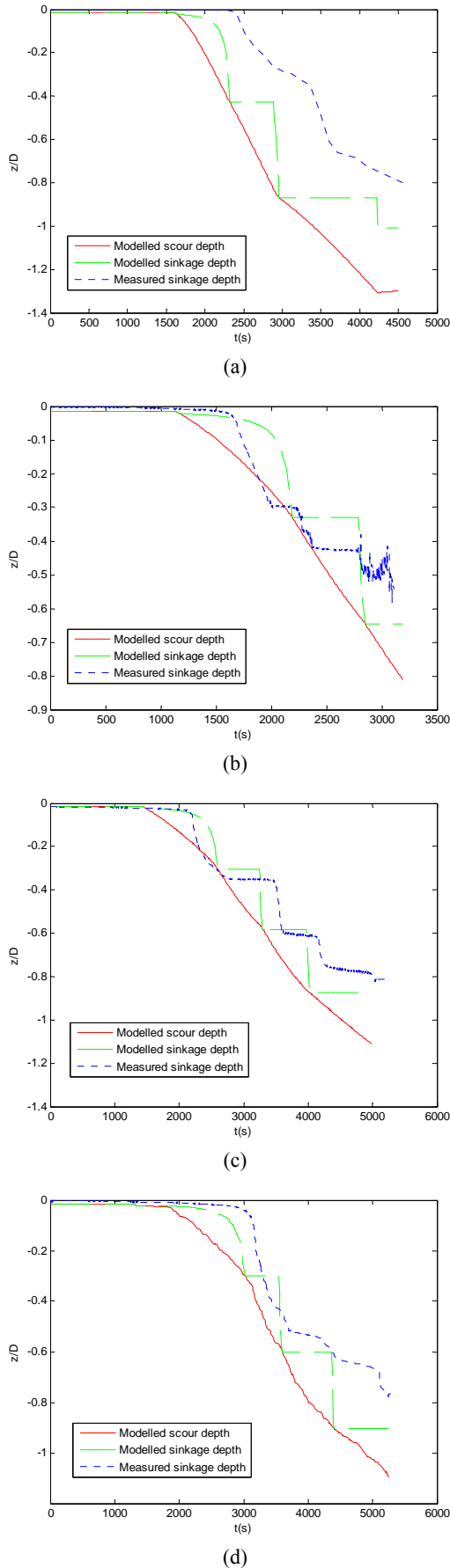


Figure 12. Comparison of model calculation with test results (a) current; (b) oscillatory flow; (c) combined regular flow; (d) combined irregular flow.

3.5 Model limitation and applicability

This model is based on the assumption of a uniform soil condition along the pipe. The soil condition in reality, however, varied in terms of the physical property and mechanical strength. This leads to the variation in sediment erodibility properties and soil bearing capacity that is related to the pipe sinkage. The other limitation in this model is the uncertainty of the onset of scour locations along a pipeline, which determines the scour propagation rate and the stress on the soil shoulders. In this model, it is assumed onset of scour initiated at the two ends of the model pipe and propagates towards the middle and there is no new span occurred during the modelled time. In the tests, however, onset of scour might also occur somewhere along the pipe and during the test. Therefore, it was hard to accurately model the pipe sinkage process without knowing the scour variation with time and along the pipe. In addition, the effects of far field sediment transportation and the associated sediment deposition around the pipe were not accounted for in this model, although observed in the tests. There is no quantitative way to incorporate these effects into the model.

Pipelines in field conditions can be up to hundreds of kilometres long. Pipeline lowering may be caused by structure deflection at free-spans or penetration at span shoulder sections. If the free-spans are relatively short and distributed intermittently along the pipeline, the pipeline lowering is predominately due to the bearing capacity failure at the span shoulders. This undulating pipe-seabed contact configuration may be caused by the pipeline being laid on an initially undulating seabed or due to the random onset of scour under moderate ocean environmental conditions. Some field survey for pipeline embedment conditions at Australia's North West Shelf provided evidence for this undulating pipeline-seabed configuration (Pinna et al. 2002). In addition, tunnel scour for real pipelines would initiate at filed joints, where the distance between field joints could be relatively small so that no significant pipeline deflection would occur over the free-span sections. The pipeline sinkage is governed by the soil bearing capacity failure simulated in this model. Therefore, the present model is applicable for these two scenarios in the field conditions.

4. CONCLUSION

O-tube pipeline stability tests showed that tunnel scour and pipe sinkage had a significant effect on the stability of pipelines with shallow initial embedment, which allow onset of scour to happen. Under the flow with realistic ramp-up rate, tunnel scour occurred at a relatively low flow velocity. The pipe sinkage process improved pipeline stability due to the sheltering effect of the scour hole.

Based on the experimental observations, the pipe sinkage mechanism was related to 3D scour and soil failure at supporting shoulders. A computation model that incorporates the 3D scour process and soil bearing failure was proposed. The model parameters were calibrated against the O-tube test results under ramp-up current, oscillatory and combined flow conditions. The model results agreed reasonably well with the test results. The pipe sinkage model provides a feasible way to quantify the self-lowering behaviour of a pipeline with undulating pipeline-seabed configuration and could be used in a new pipeline stability analysis method that takes into account the seabed mobility.

5. REFERENCES

- An, H., Luo, C., Cheng, L., and White, D. (2013) "A new facility for studying ocean-structure-seabed interactions: The O-tube", *Coastal Engineering*, Vol 82, pp88-101.
- Cheng, L., Yeow, K., Zhang, Z. and Li, F. (2014), "3D scour below pipelines under waves and combined waves and currents", *Coastal engineering*, Vol 83, 137-149.

- Chiew Y. M. (1990) "Mechanics of local scour around submarine pipelines", *Journal of Hydraulic Engineering*, 116(4), 515-529.
- Dalir, A. H. (1996) "An Experimental and Theoretical Study of the Mechanics of Self-burial of Seabed Oil and Gas Pipelines", University College, London.
- De Catania S., Breen J., Gaudin C. & White D.J., 2010. Development of multiple-axis actuator control system Int. Conf. on Physical Modelling in Geotechnics. Zurich, Switzerland, 325-330
- Det Norske Veritas (DNV) (2006) Recommended Practice, DNV-RP-F105, Free Spanning Pipelines.
- Det Norske Veritas (DNV) (2010) Recommended Practice, DNV-RP-F109, On-bottom Stability Design of Submarine Pipelines.
- Fredsøe, J., Sumer, B.M. and Arnskov, M. (1992) "Time scale for wave/current scour below pipelines", *International J. Offshore and Polar Engineering*, vol. 2, No. 2, 13-17.
- Gao, F. P. and Luo, C. (2010) "Flow-pipe-seepage coupling analysis of spanning initiation of a partially embedded pipeline", *Journal of hydrodynamics*, 22(4): 478-487.
- Gaudin, C., White, D.J., Boylan, N.P., Breen, J., Brown, T., De Catania, S., Hortin, P. 2009. A wireless high speed data acquisition system for geotechnical centrifuge testing. *Measurement Sci. and Technology*. 20 paper 095709, 11pp
- Luo, C., An, H., Cheng, L. and White, D. (2012) "Calibration of UWA's O-tube flume facility", *Proceedings of the ASME 2012 31st International Conference on Ocean, Offshore and Arctic Engineering, OMAE2012*, Rio de Janeiro, Brazil.
- Mao Y. (1988) "Seabed scour under pipelines", *Proceedings of 7th International Symposium on Offshore Mechanics and Arctic Engineering*, Houston, USA, 33-38.
- Palmer, A. C. (1996) "A flaw in the conventional approach to stability design of pipelines", *Proc. Offshore Pipeline Technology Conference*, Amsterdam, The Netherlands.
- Pinna R., Weatherald A., Grulich J., and Ronalds B. F. (2003) "Field Observations and Modelling of the Self-Burial on a North West Shelf Pipeline", *Proceedings of the 22nd International Conference on Offshore Mechanics and Arctic Engineering*, ASME, Cancun, Mexico, Vol 2, 591-599.
- Soulsby, R. (1997) *Dynamics of marine sands, A manual for practical applications*. Thomas Telford Services Ltd, London.
- Sumer, B. M., Truelsen, C., Sichmann, T. and Fredsøe, J. (2001) "Onset of scour below pipelines and self-burial", *Coastal Engineering*, Vol 42, 313-335.
- Sumer, B.M. and Fredsøe, J. (2002) *The mechanics of scour in the marine environment*, World Scientific. Singapore.
- Westgate, Z. J., White, D. J. and Randolph, M. F. (2012) "Field observations of as-laid pipeline embedment on carbonate sediments", *Geotechnique* 62, No. 9, 787-798.
- Whitehouse, R. J. S., (1998) *Scour at marine structures*, Thomas Telford.
- Zang, Z., Cheng, L. Zhao, M., Liang, D. and Teng, B. (2009) "A numerical model for onset of scour below offshore pipelines", *Coastal Engineering*. 56 (4), 458 ~ 466.
- Zang, Z., Cheng, L and Zhao, M. (2010) "Onset of scour below pipeline under combined waves and current", *Proceeding of the ASME 29th International Conference on Ocean, Offshore and Arctic Engineering*. Shanghai China. OMAE2010-20719.